International Journal of Steel Structures 16(4): 1263-1271 (2016)
DOI 10.1007/s13296-016-0073-0
ISSN 1598-2351 (Print)
ISSN 2093-6311 (Online)

International Journal of
STEEL
STRUCTURES
www.springer.com/journal/13296

Equivalent Single-Degree-Of-Freedom Analysis for Blast-Resistant Design

Kyungkoo Lee[1] and Jinwon Shin[2,*]

[1]*Associate Professor, Dankook University, Korea*
[2]*Research Professor, Dankook University, Korea*

Abstract

Protective structures subjected to blast loads are often evaluated using the equivalent single-degree-of-freedom (SDOF) analysis. Design charts for the maximum responses in the SDOF system with elastic-perfectly plastic materials are available in many textbooks and manuals such as UFC 3-340-02. These charts provide data for large scaled distances, namely, in the far field. However, few data are available for small scaled distances, namely, in the near field. This paper presents a numerical study to extend the SDOF elastic-plastic design charts to the near field. A sensitivity study for time-step size and positive phase duration is performed to obtain the optimal solutions. The proposed charts are verified using the existing design charts and the finite element methods. Recommendations for the use of the proposed charts are provided.

Keywords: SDOF analysis, Design chart, Blast load, Near field

1. Introduction

Air-blast loading is generally considered for infra-structures such as nuclear applications, petrochemical facilities, buildings and bridges. The single-degree-of-freedom (SDOF) analysis is widely used to design the protective structures subjected to blast loads. Design charts based on the SDOF analysis are available in many text-books and technical manuals such as Biggs (1952), TM5-1300 (Department of the Army, Navy and Air Force 1990), UFC 3-340-02 (DoD 2008), Cormie *et al.* (2009), and Dusenberry (2010).

The SDOF design charts, as shown in Fig. 1, provide maximum responses of the SDOF system as a function of variables of positive phase duration divided by natural period (t_d/T_n) and maximum resistance divided by equivalent peak load (R_m/F_e). Assumptions made for the use of the equivalent SDOF charts for blast-resistance design are that (1) structures show elastic-perfectly plastic behavior, (2) loads are applied uniformly to structures, and (3) the loading shape is triangular or rectangular, where the triangular loading will be more appropriate due to its shape similar to the practical blast loading.

Blast loading is determined based on empirical charts available in UFC 3-340-02 (DoD, 2008), which provides air-blast parameters such as reflected peak overpressure, reflected impulse, positive phase duration, shock-front arrival time, and reflection coefficient to include the effect of angle of incidence. These empirical charts to determine blast loading have been implemented in ConWep (Hyde 1992) and are utilized for blast design and analysis. The UFC 3-340-02 charts may underpredict blast pressures and impulses very close to the face of the charge (Shin et al. 2015), but this is not considered in this study.

The SDOF design charts, described above, are useful for design of protective structures subjected to blast loading. However, in the near field, the data of the SDOF responses are not sufficient to yield the responses of structures because the two non-dimensional variables, used to pick the maximum responses, as described previously, are not within the charts in the near field. This paper presents a study to update the SDOF elastic-plastic design graphs, thereby covering the near-field range. The updated charts are developed with the central difference method (CDM) (e.g., Chopra, 2012). A verification study is performed using UFC 3-340-02 (DoD, 2008) and a finite element code LS-DYNA (LSTC, 2013) to prove the robustness of the proposed calculations to develop the charts.

Received February 1, 2016; accepted June 28, 2016;
published online December 31, 2016

*Corresponding author
Tel: +82-31-8005-3745, Fax: +82-31-8021-7225
E-mail: jshin@dankook.ac.kr

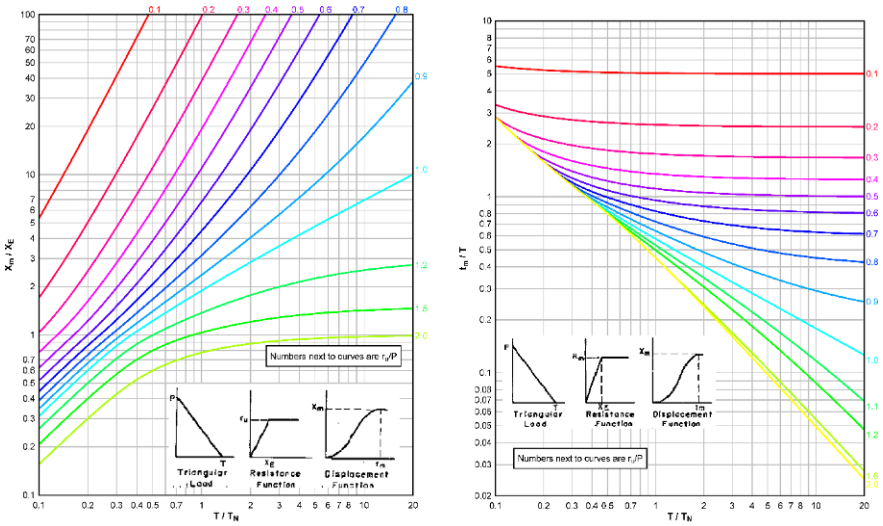

(a) x_m/x_{el} (b) t_m/t_d

Figure 1. UFC 3-340-02 (DoD 2008) design charts for maximum responses in elastic-plastic SDOF system under triangular loading.

2. Equivalent SDOF Analysis for Blast-resistant Design

2.1. Equivalent SDOF analysis

A typical equivalent single-degree-of-freedom (SDOF) analysis for a beam with simply-supported condition is illustrated in Fig. 2. Blast pressures acting on the beam are assumed uniform. The simply-supported beam under uniform pressures can be transformed into an equivalent SDOF system. The transformation factors for mass, K_M, and for load, K_L, are provided in Table 1 per UFC 3-340-02 (DoD, 2008). The established SDOF system gives an equation of motion, as shown in Eq. (1), which leads to the maximum displacement and the corresponding time, as shown in Fig. 1, through time-history analysis. Damping of structures for the high-frequency and short-duration blast loads is ignored.

$$M_e\ddot{x} + c\dot{x} + k_e x = F_e(t) \tag{1}$$

The SDOF analysis assumes that the system shows elastic-perfectly plastic deformation. The resistance function of the system is expressed using bilinear curve, as shown in Fig. 3. For the simply-supported beam in Fig. 2, the maximum resistance, R_m, and the stiffness, k, are computed

Table 1. UFC 3-340-02 transformation factors for simply supported beam

Strain rage	Elastic	Plastic
K_L	0.64	0.50
K_M	0.50	0.33

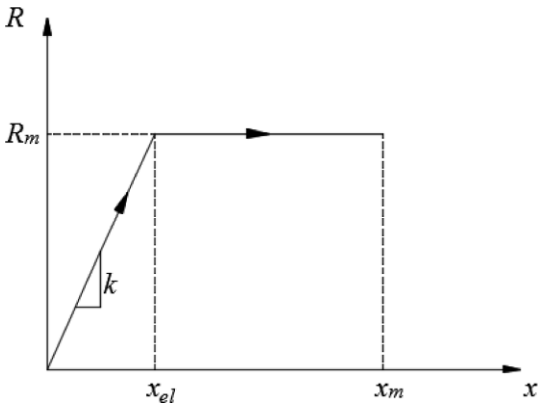

Figure 3. Resistance function.

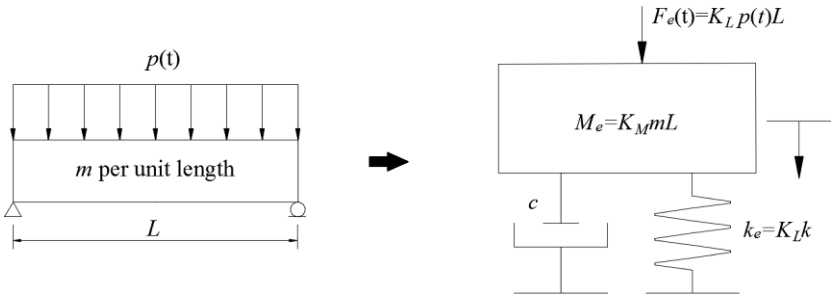

Figure 2. Equivalent single-degree-of-freedom analysis.

as 8 M_p/L and 384 $EI/5L^3$, respectively, where M_p is the plastic moment, E, is the elastic modulus, and I is the moment of inertia.

2.2. Blast analysis using SDOF approach

Air-blast parameters such as overpressure and impulse are defined as a function of scaled distance, Z, where $Z=R/W^{1/3}$, R is standoff distance, and W is weight of explosive. The SDOF charts of Fig. 1, used to obtain the maximum responses of structures subjected to shock loads, are available for design at large scaled distances representing far-field detonations. However, there is few data in the charts for small scaled distance representing near-field detonations. A sample steel component with dimensions of 0.2×0.2×4 m subjected to a triangular pulse is prepared to clarify this.

The steel component is designed with a plastic section modulus similar to a typical steel section of W1474 and with a length of 4 m. The properties of the steel component is provided in Table 2. The input parameters of R_m/F_e and t_d/T_n are generated as a function of scaled distance, Z, in the range $0.053<Z<20$ m/kg$^{1/3}$. Where the lower boundary of Z (=0.053 m/kg$^{1/3}$) represents the face of the charge. The maximum load, F_e, and the positive phase duration, t_d, are determined using charts available in UFC 3-340-02 for air-blast parameters. The lower limits of R_m/F_e and t_d/T_n of the UFC 3-340-02 SDOF elastic-plastic charts are 0.1 and 0.1, respectively, as shown in Fig. 1. However, the calculated R_m/F_e and t_d/T_n in Fig. 4 for small scaled distances are less than the lower limits, in the range $Z<0.67$ m/kg$^{1/3}$ for R_m/F_e and $Z<2.8$ m/kg$^{1/3}$ for t_d/T_n, although the UFC 3-340-02 charts cover the far-field ranges. This indicates that the existing SDOF design charts needs to be extended for assessment of structural responses to the near field, noting that the focus on security design of mission-critical structures is the near field.

Table 2. Properties of a sample steel component

Properties	Values
Section dimension (m)	0.2×0.2
Length, L (m)	4
Maximum resistance, R_m (kN)	1,400
Stiffness, k (kN/m)	32,000
Natural period, T_n (sec)	0.0335
Density (kg/m^3)	7830
Elastic modulus, E (GPa)	200

3. Proposed SDOF Calculations and Charts

The SDOF calculations and design charts are proposed to provide the maximum displacement and the corresponding time for triangular loading for near-field detonations of high explosives. Equations of motion for a simply supported component with bilinear resistance function are constructed, and they are implemented in a Matlab code using the central difference algorithms. Design charts are developed using the proposed numerical calculations to provide data for t_d/T_n and R_m/F_e down to 0.001 and 0.001, respectively. This range is considered sufficient to cover the near-field range based on Fig. 4. A sensitivity analysis is performed to obtain the optimal numerical solutions independent of time-step size and positive phase duration. The proposed design charts are also verified using the data in UFC 3-340-02 (DoD 2008) and a code LS-DYNA (LSTC 2013).

3.1. System resistance and loading

The resistance function of the SDOF elastic-perfectly plastic system is established using a bilinear curve, shown in Fig. 3. As there is no negative phase in the loading, the maximum responses would be obtain during the two stages. The resistance, $R(x)=kx$ for $0<x<x_{el}$ and $R(x)=R_m$ for $x_{el}<x<x_m$, where x_{el} is yield displacement, x_m is maximum displacement, and R_m and k are described previously. The triangular loading function, $F(t)=F(1-t/t_d)$ for $t<t_d$ and $F(t)=0$ for $t>t_d$, where F is the maximum load, and t_d is positive phase duration, where $t_d=2I_r/P_r$, and I_r and P_r are reflected impulse, and reflected peak overpressure determined per UFC 3-340-02.

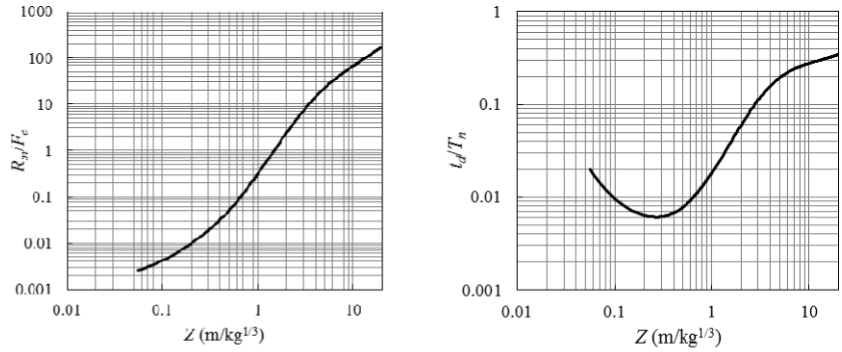

(a) R_m/F_e versus Z (b) t_d/T_n versus Z

Figure 4. R_m/F_e and t_d/T_n as a function of scaled distance, Z, for a sample steel component.

3.2. Equations of motion

The equations of motion in Eq. (1) is modified with consideration of resistance function and triangular loading described in Section 3.1. Two cases are considered: (1) Case I: t_{el} is less than t_d and (2) Case II: t_{el} is larger than t_d. The effect of damping is neglected, as described previously. The initial conditions are assumed to be zero.

When $t_{el}<t_d$ (Case I), the equation of motion in the first stage, namely, $x>x_{el}$, is:

$$m\ddot{x}(t)+kx(t)=F(t) \quad \text{for } t<t_{el}<t_d \tag{2}$$

In the second and third stages ($x>x_{el}$), the equations of motion are

$$\begin{aligned} &m\ddot{x}(t)+R_m=F(t) \quad \text{for } t_{el}<t<t_d \\ &m\ddot{x}(t)+R_m=0 \quad \text{for } t_{el}<t_d<t \end{aligned} \tag{3}$$

Equations of motion when $t_{el}>t_d$ (Case II), are similarly generated. In the first and second stages ($x<x_{el}$), the equations of motion are:

$$\begin{aligned} &m\ddot{x}(t)+kx(t)=F(t) \quad \text{for } t<t_d \\ &m\ddot{x}(t)+kx(t)=0 \quad \text{for } t_d<t<t_{el} \end{aligned} \tag{4}$$

In the third stage ($x<x_{el}$), the equation of motion is:

$$m\ddot{x}(t)+R_m=0 \quad \text{for } t_{el}<t \tag{5}$$

These constructed equations of motion are solved numerically using the central difference method (CDM) in the following section.

3.3. Numerical algorithms

The central difference method (CDM, Chopra 2012) is a numerical approximation of derivatives of displacement with respect to time. Calculations for the initial condition of the SDOF elastic-plastic system are first made. Acceleration, $\ddot{x}_0$, at $t=0$ is:

$$\ddot{x}_0=\frac{F_0-kx_0}{m} \tag{6}$$

A fictitious initial condition, x_{-1}, to compute x_1 is:

$$x_{-1}=x_0-\Delta t\dot{x}_0+\frac{\Delta t^2}{2}\ddot{x}_0 \tag{7}$$

A constant, a, which is defined for ease of calculation:

$$a=\bar{k}=\frac{m}{\Delta t^2} \tag{8}$$

Velocity and acceleration at time i, $\dot{x}_i$ and $\ddot{x}_i$, respectively, are calculated as:

$$\dot{x}_i=\frac{x_{i+1}-x_{i-1}}{2\Delta t} \quad \text{and} \quad \ddot{x}_i=\frac{x_{i+1}-2x_i+x_{i-1}}{\Delta t^2} \tag{9}$$

Then, the equation of motion is solved following step-by-step procedure with CDM. Four different shapes of equations in Eqs. (2) through (5) are computed. For Eqs. (2) and (4), $m\ddot{x}(t)+kx(t)=F(t)$ with Eq. (9) leads to:

$$x_{i+1}=\frac{\bar{F}_i}{\bar{k}} \quad \text{and} \quad \bar{F}_i=F_i-ax_{i-1}-(k-2a)x_i \tag{10}$$

where $\bar{k}$ is described previously. In Eq. (4), $m\ddot{x}(t)+kx(t)=0$ with Eq. (9) leads to:

$$x_{i+1}=\frac{\bar{F}_i}{\bar{k}} \quad \text{and} \quad \bar{F}_i=-ax_{i-1}-(k-2a)x_i \tag{11}$$

For Eq. (3), $m\ddot{x}(t)+R_m=F(t)$ with Eq. (9) gives

$$x_{i+1}=\frac{\bar{F}_i}{\bar{k}} \quad \text{and} \quad \bar{F}_i=F_i-R_m-ax_{i-1}+2ax_i \tag{12}$$

Lastly, in Eqs. (3) and (5), $m\ddot{x}(t)+R_m=0$ with Eq. (9) results in:

$$x_{i+1}=\frac{\bar{F}_i}{\bar{k}} \quad \text{and} \quad \bar{F}_i=R_m-ax_{i-1}+2ax_i \tag{13}$$

The numerical procedures discussed in this section are summarized in Table 3. The SDOF elastic-plastic response charts calculated using CDM per Table 3. Sensitivities of time-step size and positive phase duration to the numerical solutions are studied in the following section.

3.4. Sensitivity study for time-step size and positive phase duration

A sensitivity study of time step size and positive phase duration is performed to obtain a reasonable balance between solution accuracy and computation expense. Three time-step sizes, dt, of 10^{-3}, 10^{-4} and 10^{-5} sec and two positive phase durations, t_d, of 0.1 and 0.001 sec are considered. Numerical simulations are performed for t_d/T_n=0.001 and 20 and R_m/F_e=0.001 and 2.

Figure 5 presents results for the three time-step sizes for t_d=0.1. The results are generated as displacement, x, histories normalized by yield displacement, x_{el}, as a function of time, t, normalized by the positive phase duration, t_d. For all considered situations, the results for $dt=10^{-4}$ and 10^{-5} are essentially identical. Accordingly, the optimal time-step size for t_d=0.1 to develop the SDOF charts are chosen to be $dt=10^{-4}$.

The effect of positive phase duration on the results is studied using the time-step converged solutions. Figure 6 presents results for t_d=0.001 and 0.1 sec. The results are effectively identical independent of positive phase duration, noting that the results for t_d=0.001 sec converged with $dt=10^{-6}$. The SDOF elastic-plastic responses are therefore calculated using t_d=0.1 sec and $dt=10^{-4}$ sec. The proposed design charts for SDOF elastic-plastic system under

Table 3. Step-by-step procedure for numerically solving equations of motion with CDM for SDOF elastic-plastic system

I. Initial calculation

Acceleration at $t = 0$	$\ddot{x}_0 = \dfrac{F_0 - kx_0}{m}$
Initial condition	$x_{-1} = x_0 - \Delta t\dot{x}_0 + \dfrac{\Delta t^2}{2}\ddot{x}_0$
Constant	$a = \bar{k} = \dfrac{m}{\Delta t^2}$

II. Computation for time step i

Case 1 ($t_{el} < t_d$)	Stage 1: $x < x_{el}$, $t < t_{el} < t_d$	$\bar{F}_i = F_i - ax_{i-1} - (k-2a)x_i$
	Stage 2: $x > x_{el}$, $t_{el} < t < t_d$	$\bar{F}_i = F_i - R_m - ax_{i-1} + 2ax_i$
	Stage 3: $x > x_{el}$, $t_{el} < t_d < t$	$\bar{F}_i = R_m - ax_{i-1} + 2ax_i$
Case 2 ($t_{el} > t_d$)	Stage 1: $x < x_{el}$, $t < t_d$	$\bar{F}_i = F_i - ax_{i-1} - (k-2a)x_i$
	Stage 2: $x < x_{el}$, $t_d < t < t_{el}$	$\bar{F}_i = -ax_{i-1} - (k-2a)x_i$
	Stage 3: $x > x_{el}$, $t_{el} < t$	$\bar{F}_i = R_m - ax_{i-1} + 2ax_i$
Displacement at t_{i+1}		$x_{i+1} = \dfrac{\bar{F}_i}{\bar{k}}$
Velocity and acceleration at t_i		$\dot{x}_i = \dfrac{x_{i+1} - x_{i-1}}{2\Delta t}$ & $\ddot{x}_i = \dfrac{x_{i+1} - 2x_i + x_{i-1}}{\Delta t^2}$

III. Go to step II with $t_{i+1} = t_i + \Delta t$ and repeat

IV. Terminated at $t_d / T_n = 10$

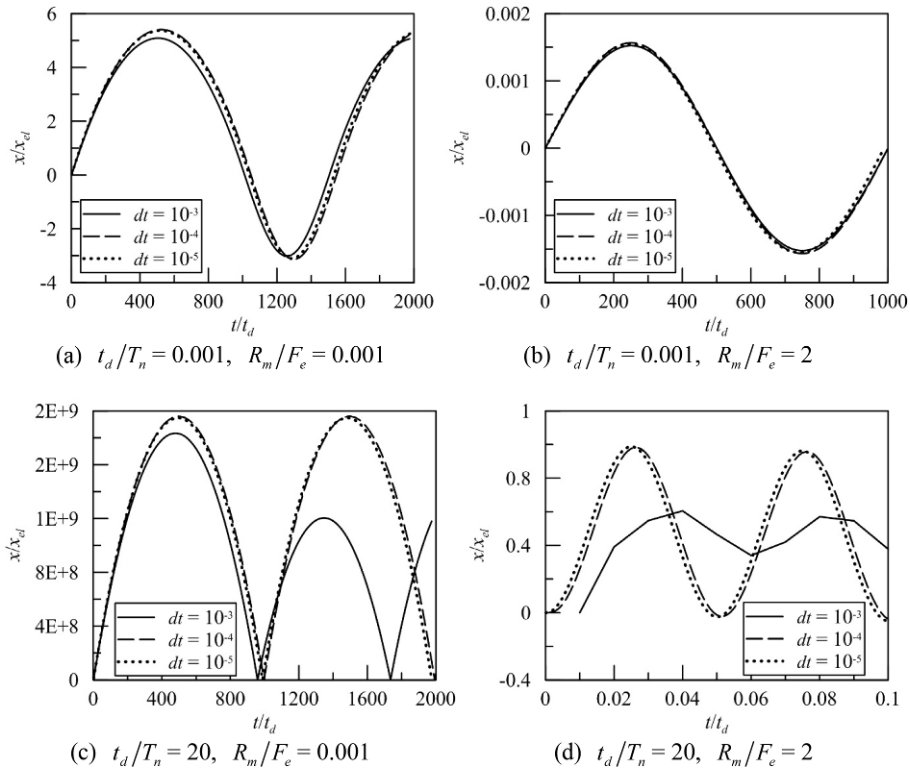

(a) $t_d/T_n = 0.001$, $R_m/F_e = 0.001$ (b) $t_d/T_n = 0.001$, $R_m/F_e = 2$

(c) $t_d/T_n = 20$, $R_m/F_e = 0.001$ (d) $t_d/T_n = 20$, $R_m/F_e = 2$

Figure 5. Sensitivity study of time step size with t_d=0.1 sec.

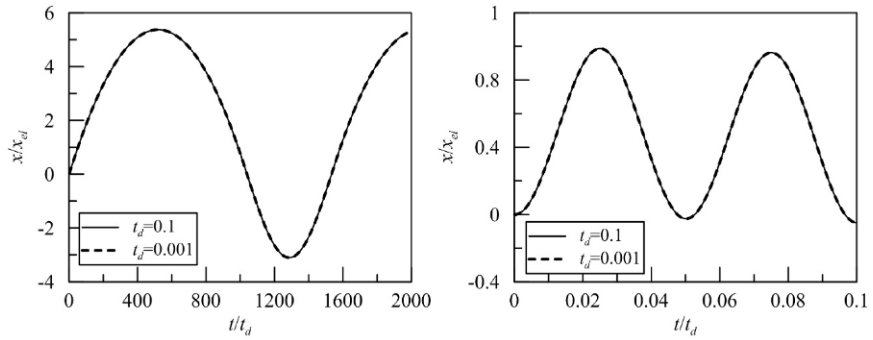

(a) t_d = 0.001 sec (b) t_d = 0.1 sec

Figure 6. Sensitivity study of positive phase duration, t_d

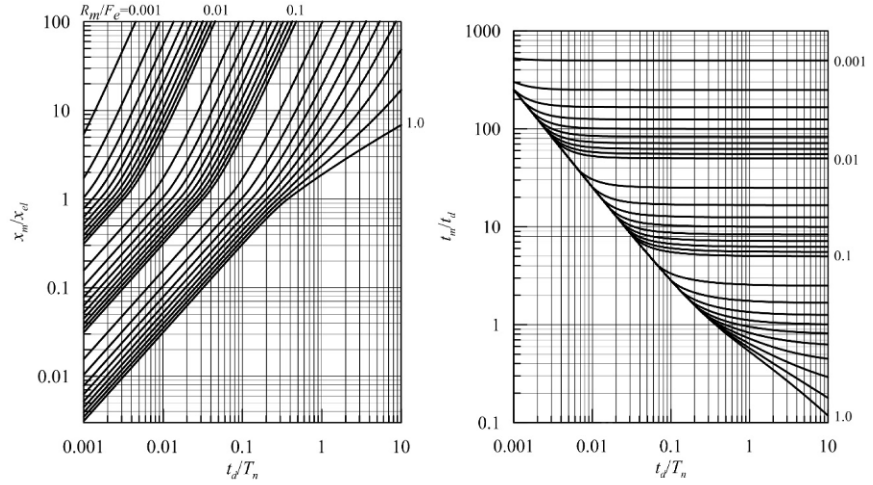

(a) x_m/x_{el} (b) t_m/t_d

Figure 7. Proposed SDOF elastic-plastic design charts for triangular loading.

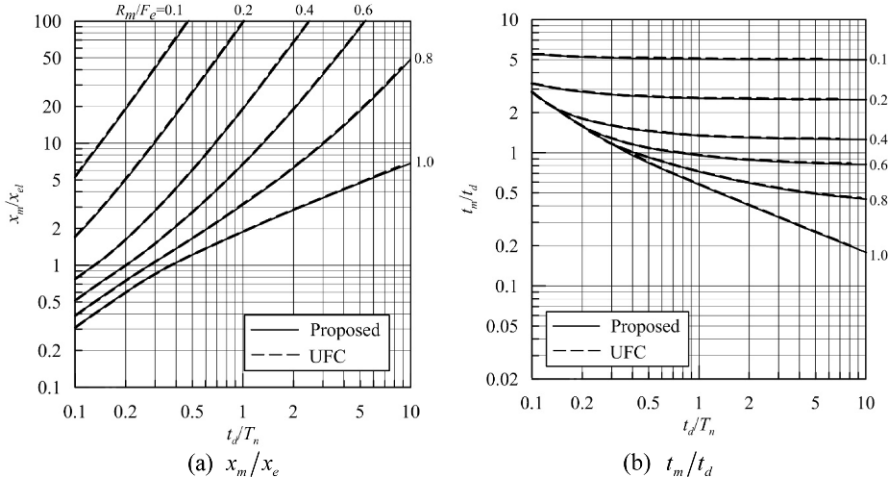

(a) x_m/x_e (b) t_m/t_d

Figure 8. Verification of proposed charts based on UFC 3-340-02.

triangular loading are presented in Fig. 7.

3.5. Verification study of proposed charts

A verification study for the proposed charts is performed to demonstrate the robustness of the proposed SDOF calculations per Table 3. The proposed charts are compared to data in UFC 3-340-02, as shown in Fig. 8 in the range $0.1<t_d/T_n<10$ for R_m/F_e=0.1, 0.2, 0.4, 0.6, 0.8 and 1.0. The number of data point of t_d/T_n is 1000. The proposed charts and the UFC 3-340-02 data are virtually identical.

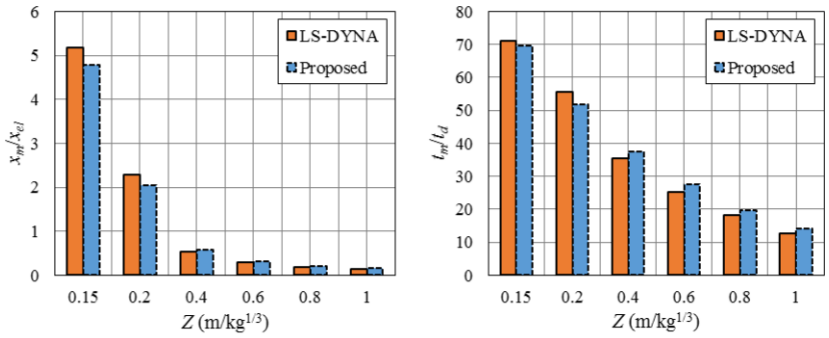

Figure 9. Verification of proposed charts with comparison to LS-DYNA results.

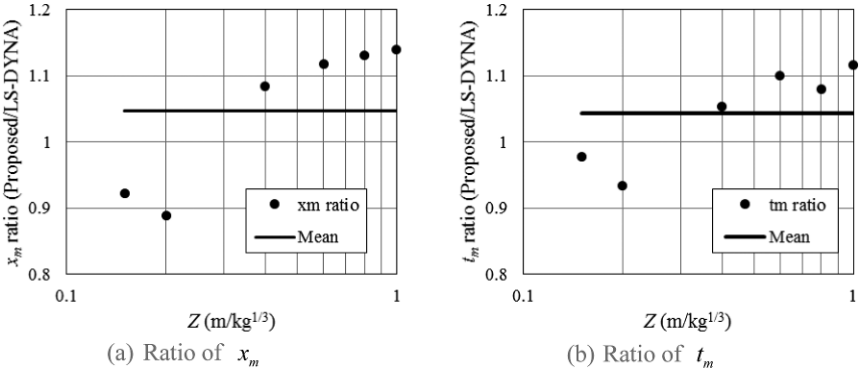

Figure 10. Statistical analysis for ratios of x_m and t_m.

The proposed charts are therefore considered verified for larger scaled distances (Fig. 4).

For verification in the smaller scaled distances, a finite element analysis is conducted. The sample steel component, introduced in Section 2 with Table 2, having dimensions of 0.20.24 m and a triangular pulse is modeled in LS-DYNA (LSTC 2013). Analysis is performed for six scaled distances, Z, of 0.15, 0.2, 0.4, 0.6, 0.8 and 1 m/kg$^{1/3}$. The lower bound of Z (=0.15 m/kg$^{1/3}$) is selected because UFC 3-340-02 provides overpressure histories at Z>0.147 m/kg$^{1/3}$. The upper bound of Z of 2 m/kg$^{1/3}$ is taken, noting that t_d/T_n of 0.1, which is the smallest value in the UFC 3-340-02 charts, corresponds to Z=2.8 m/kg$^{1/3}$ (Fig. 4(b)).

Results are presented in Fig. 9. The LS-DYNA predictions and the proposed calculations are in good agreement for both x_m/x_{el} and t_m/t_d. A statistical analysis is performed to complement this verification work. Ratios between the results of the proposed charts and LS-DYNA are calculated for all considered scaled distances, as shown in Fig. 10. Then, the statistical measures of the mean, standard deviation (SD) and coefficient of variation (CV) for these ratios are computed using standard statistical functions, as presented in Table 4. The mean values for the ratios of x_m and t_m are close to 1.0, which indicates that the proposed predictions and the LS-DYNA calculations are, in a mean sense, very similar. Also, the calculated CVs are approximately less than 10, indicating the ratios are very stable around the mean. The proposed charts are thus considered verified for smaller scaled distances.

Table 4. Statistical analysis for ratios of x_m and t_m

Measures	Ratio of x_m	Ratio of x_m
Mean	1.048	1.044
SD	0.112	0.0724
CV	10.7	6.94

Table 5. Sample calculations for the proposed charts

Results	t_d/T_n=0.01		t_d/T_n=1	
	R_m/F_e=0.01	R_m/F_e=1	R_m/F_e=0.01	R_m/F_e=1
x_m/x_{el}	5.40	0.0313	48,427	1.88
x_{el}	0.0253	2.533	2.533×10^{-6}	2.533×10^{-4}
x_m	0.137	0.0793	0.123	0.000477
t_m/t_d	52.7	25.3	49.9	0.576
t_d	0.1	0.1	0.1	0.1
t_m	5.27	2.53	4.98	0.0576

4. Sample Calculations

Table 5 presents results of sample calculations for analysts to use the proposed charts. The positive phase duration, t_d, of 0.1 sec is used. The maximum equivalent load, F_e, and the equivalent mass, M_e, are assumed here

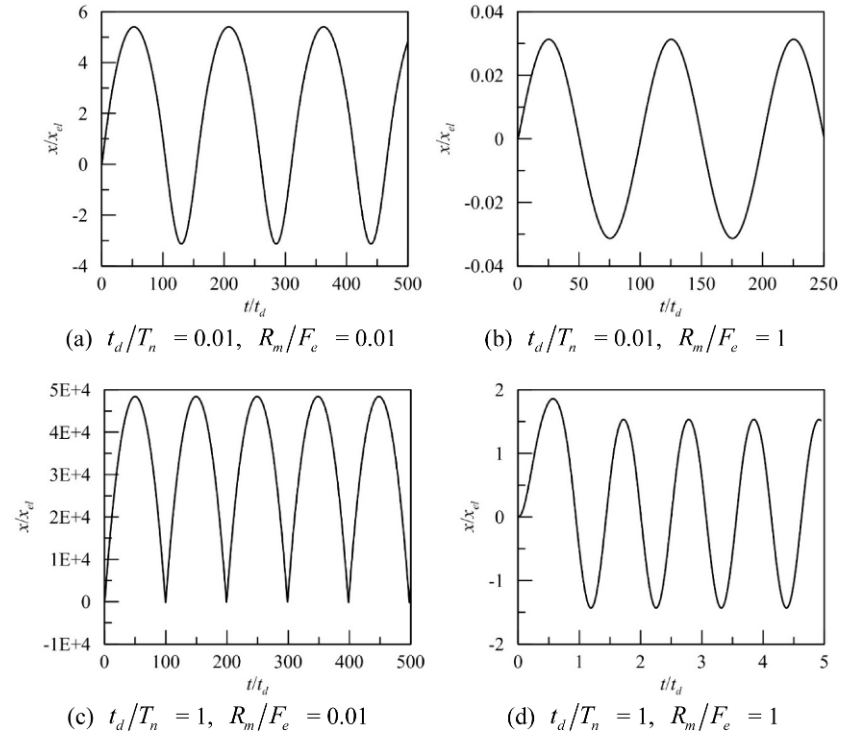

Figure 11. Response histories for sample calculations.

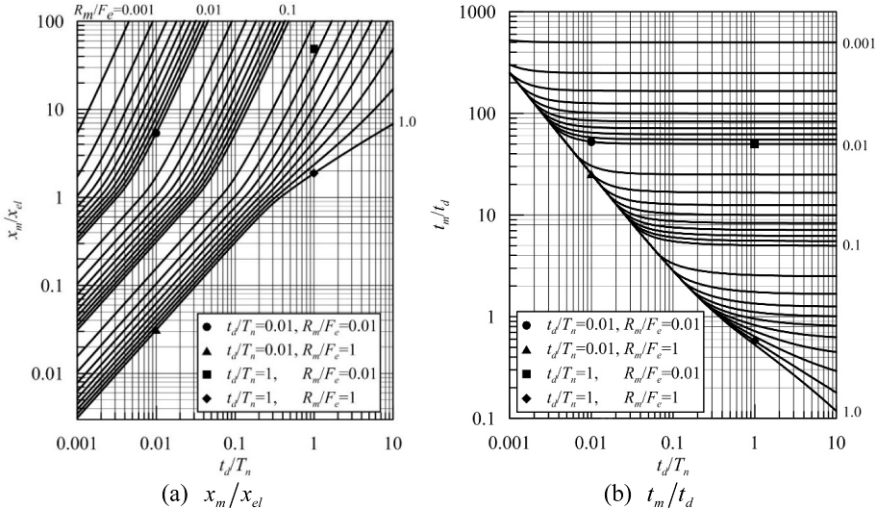

Figure 12. Use of proposed charts.

1.0 and 1.0, respectively. Sample calculations are performed for t_d/T_n=0.01 and 1 and R_m/F_e=0.01 and 1. All parameters in the table were defined previously. Response histories of x/x_{el} as a function of t/t_d for each are presented in Fig. 11. The sample results compared to the proposed charts are provided in Fig. 12.

5. Concluding Remarks

This paper proposes updated design charts for maximum responses of elastic-plastic SDOF system for blast-resistant design with an emphasis on the near field. The proposed charts enable predictions of the maximum displacement and the corresponding time in the range $0.001<t_d/T_n<10$ and $0.001<R_m/F_e<1$. Numerical algorithms are established to develop the charts using finite difference calculations. A sensitivity study shows the calculated data independent of time-step size and positive phase duration. The charts are also verified using existing data such as those in UFC 3-340-02 and finite element code. Since the charts in UFC 3-340-02 provide data only for far-field detonations, it is suggested to use the proposed charts for near-field blast events.

Acknowledgment

The present research was conducted by the research fund of Dankook University in 2014.

References

Biggs, J. M. (1964). *Introduction to Structural Dynamics*. McGraw-Hill, NY.

Chopra, A. K. (2012). *Dynamics of Structures: Theory and Applications to Earthquake Engineering, 4th edition*. Prentice Hall, Upper Saddle River, NJ.

Cormie, D., Mays, G. and Smith, P. (2009). *Blast Effects on Buildings, 2nd Ed*. London: Thomas Telford.

Department of the Army, Navy and Air Force. (1990). S*tructures to Resist the Effects of Accidental Explosions (with Addenda)*. Army Technical Manual (TM 5-1300), Navy Publication (NAVFAC P-397), Air Force Manual (AFM 88-22), Revision 1. Washington, DC.

DoD. (2008). *Unified Facilities Criteria (UFC): Structures to Resist the Effects of Accidental Explosions (UFC 3-340-02)*. Departments of Defense, Washington, DC.

Dusenberry, D. O. (2010). ed. *Handbook for Blast-Resistant Design of Buildings*. Wiley, Hoboken, NJ.

Hyde, D. W. (1992). *ConWep: Conventional Weapons Effects (Application of TM 5-855-1)*. US Army Corps of Enigneers, Waterways Experiment Station, Vicksburg, MS.

LSTC. (2013). *LS-DYNA Keyword User's Manual Ver. R7.0*. Livermore Software Technology Corporation, Livermore, CA.

Shin, J., Whittaker, A. S., Cormie, D., and Wilkinson, W. (2014). "Numerical modeling of close-in detonations of high explosives." *Engineering Structures*, 81, pp. 88-97.

Shin, J., Whittaker, A. S., Cormie, D. (2015). "Incident and normally reflected overpressure and impulse for detonations of spherical high explosives in free air." *Journal of Structural Engineering*, 10.1061/(ASCE)ST. 1943-541X.0001305 , 04015057.

Smith, P. D. and Hetherington, J. G. (1994). *Blast and Ballistic Loading of Structures*. Butterworth-Heinemann, Oxford; Boston.